

CO₂ Laser Induced Chain Reaction of C₂F₄ + CF₃I

Gong Mengxiong,[†] W. Fuss,* and K. L. Kompa

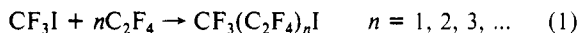
Max-Planck Institut für Quantenoptik, D-8046 Garching, Federal Republic of Germany
(Received: September 20, 1989; In Final Form: December 21, 1989)

A pulsed CO₂ laser was used to induce the telomerization of CF₃I with C₂F₄ in gas phase. This is an exothermic radical chain reaction, producing CF₃(CF₂)_nI with low *n*. A problem, previously considered unresolvable, exists at low pressure: Good primary quantum yield is in conflict with long chain length; for kinetic reasons the chain length is short, if initially a high yield of radicals is generated by IR multiphoton dissociation. Radical dimers dominate in this case. To avoid this undesired direction of the reaction, we applied a novel method: At high pressure the radicals are generated with delay only, so that their instantaneous concentration is always small. At 3 bar we attained quantum yields of 0.2 for the desired iodides, with selectivity of 80%. This good selectivity is a consequence of the second-order termination, according to our analysis. The quantum yield is 100 times larger than previously reported for a CO₂ laser induced reaction. It can be raised even more, if the exothermicity is used for further propagation. We only came close to this ignition threshold. With more laser energy in longer pulses, it could be reached.

1. Introduction

With pulsed CO₂ lasers, many molecules can be easily dissociated by multiphoton absorption. Typically, the degree of dissociation is of the order of 10%, if the average absorption is about 10–20 photons per molecule. This corresponds to a quantum yield of 0.01–0.005. Although for some processes like isotope separation this is acceptable and although CO₂ laser photons are cheap, higher quantum yields would be desirable for some other products. It is natural in this context to think of radical chain reactions. It is true that such laser-induced reactions become more and more similar to thermally induced reactions, the longer the chain length and the higher the quantum yield. However, because of the reduced costs, minor differences could be decisive to favor the laser-induced process.

We investigated the insertion of C₂F₄ into the C–I bond of CF₃I:



This is an exothermic radical chain reaction. It is a prototype of the so-called telomerization. A monograph is available about such reactions.¹ They can be induced thermally¹ or photochemically.^{1,2} The chain propagation in (1) and similarly in all telomerizations consists of the growth steps (addition of C₂F₄ to the radicals) and the chain transfer (transfer of I from CF₃I to the CF₃(CF₂)_n radical). Bagratashvili et al.³ briefly mention an investigation of a similar CO₂ laser induced reaction with CF₃Br instead of CF₃I, which was, however, carried out at low pressure (1.3 mbar of CF₃Br + 67 mbar of C₂F₄). The quantum yields were not reported, but were probably very small. In fact, when we carried out our reaction (iodide instead of bromide) at such a low pressure (sections 5 and 6), we found very short kinetic chain lengths. (That is, only a few iodide molecules were produced for each primary CF₃ radical. Most of the latter were converted to C₂F₆.) Since the Br atom transfer is slower than the I atom transfer, in ref 3 longer molecule chains (so, heavier molecules) were produced, in spite of the short kinetic chain length.

In IR laser induced chain reactions a conflict is expected: Usually kinetic chain lengths are inversely proportional to the radical concentrations [R], since the common chain termination is radical recombination, which is of second order in [R], whereas the propagation is of first order only. In UV photochemistry and generally in all one-photon dissociation processes it is easy to generate small [R] simply by using small intensities. In IR multiphoton dissociation, however, lowering the intensities always drastically reduces the quantum yields of the primary dissociation. It is the product of primary quantum yield times the chain length which determines the yield of chain propagation products. So

at first sight it seems that these yields can never be high. Although in principle this problem could be circumvented by using very small CF₃I pressures, these pressures would be too low for practical purposes.

In contrast to low pressure which implies nearly collisionless conditions, at high pressure the dissociation of CF₃I is a thermal process and a large fraction of the CF₃ radicals are released only after the laser pulse. So the instantaneous radical concentration is smaller and the chain length longer. The yield depends on the reaction time and therefore on the cooling rate. Cooling by thermal conductivity is slower, the higher the pressure. (Thermal radiation and convection can be neglected.) Since our reaction is exothermic, we might in addition even profit from the heat of reaction. It is expected that above a pressure threshold (ignition condition) the heat of reaction, released per time unit, can compensate the heat loss. Then the reaction will be self-sustained and the quantum yield can be unlimited. In this work, we approached this threshold. Quantum yields up to 100 times higher than at low pressure have been attained.

We observed selectivities for the desired products, which are surprising in view of the high temperatures involved (≈1000 K). We show however, that high pressure and, to a limited extent, high temperature favor good selectivities, if the propagation and termination reactions are of first and second order in the radical concentration, respectively.

In initial experiments we irradiated the axis of a cylindrical cell, which contained a gas mixture of CF₃I + C₂H₄.⁴ The ignition threshold was not reached, although we expected it on the basis of estimations of heat conduction. Since the latter is not known at high temperature, we decided to measure the temporal evolution of the temperature. To do this, we illuminated the full volume of a small cell (2 cm³) and measured the pressure with a fast pressure gauge. In numerical calculations of heat conduction, matched to these experimental data, we found the temperature dependence (∝ T²) of the temperature conductivity. This was then used to calculate the reaction in larger cells, which suffer less from heat conduction, because the walls are not so close to the hot zone. We obtained, however, only qualitative agreement. Reasons for the deviations are considered.

In this work we used C₂F₄ instead of C₂H₄. The fluorinated system allows higher temperatures and thus higher reaction rates,

(1) Starks, Ch. M. *Free Radical Telomerization*; Academic Press: New York, 1974.

(2) Zhang, Linyang; Fuss, W.; Kompa, K. L. Submitted for publication in *Ber. Bunsen Phys. Chem.*

(3) Bagratashvili, V. N.; Kuzmin, M. V.; Letokhov, V. S. *J. Phys. Chem.* **1984**, *88*, 5780.

(4) Fuss, W.; Gong, Mengxiong; Kompa, K. L.; Zhang, Linyang *Spectrochim. Acta* **1987**, *43A*, 193.

[†] Present address: Department of Chemistry, University of Houston, Houston, TX 77204-5641.

TABLE I: Geometry of the Cells Used

cell	A	B	C
length, cm	1	1	10
radius, mm	8	4	17

and it is also slightly more exothermic.

2. Experimental Section

A home-made atmospheric pressure CO₂ laser was used. Its pulses had up to 5 J of energy and consisted of a 100-ns (half-width) spike with 30% of the energy and a 3- μ s (full length) tail. For most experiments (at 0.8 J/cm²) the radiation was used unfocused. In some other cases we used a lens of 1 m focal length and placed the irradiation cells near the focus.

We employed the laser lines 9P28 (1039.4 cm⁻¹) and, less often, 9P40 (1027.4 cm⁻¹). The first one is in the short-wavelength wing, and the second one in the center, of the $\nu_2 + \nu_3$ band of CF₃I.⁵ Results did not depend on the wavelength but only on the absorbed energy. Absorptions were determined from incident and transmitted energies of the cells. On 9P28 we found adsorption cross sections of 4.5×10^{-19} to 2.0×10^{-19} cm² at 0.9 to 2.6 J/cm², respectively, at 100 mbar of CF₃I and 1.2 times higher values at 1 bar CF₃I. These numbers correspond to 7–8.7 photons/molecule of the gas mix ([CF₃I]:[C₂F₄] = 1:2), absorbed on the average. The dissociation limit of CF₃I corresponds to 18 photons. On 9P40 the absorption is stronger by about 30%.

Cylindrical cells with different sizes have been used (Table I). The cells, made of stainless steel, were equipped with two KCl windows. A small-volume (0.3 cm³) side arm of cell A contained a piezo-resistive pressure probe (Kistler) with time resolution less than 1 ms. The time-dependent pressure p and temperature T are related via a spatial average of T^{-1} . In the general gas equation (k_B = Boltzmann constant)

$$p = nk_B T \quad (2)$$

T and the molecular number density n vary over the cell, whereas p does not. From constancy of number of molecules there follows (integrals over the cell volume, subscript 0 denotes time 0)

$$n_0 V = \int n dV \quad (3)$$

$$p_0 (k_B T_0)^{-1} V = p \int (k_B T)^{-1} dV \quad (4)$$

$$p/p_0 = V / (T_0 \int T^{-1} dV) \quad (5)$$

CF₃I was from Kali-Chemie with a stated purity of 99%. C₂F₄ was prepared by vacuum pyrolysis of its polymer.⁶ According to IR spectra, it contained about 7% CF₃CF=CF₂ and 3% cyclo-C₄F₈. Both gases were used without further purification; the impurities were subtracted from the yields. The number of pulses was chosen so that the conversion was always between 20 and 50%.

The partial pressures of the reagents along with the product C₂F₆ were monitored by infrared spectroscopy before and after laser irradiation. The product yields were determined by gas chromatography combined with mass spectrometry. Separation was accomplished by a column of 0.2 mm \times 25 m, coated with 5% phenylmethylsilicone with the temperature increasing from 30 to 200 °C in 17 min, with the exception of C₂F₄ and C₂F₆, which we separated in the same column at -80 °C when desired. The mass spectrometer response (range 20–600 mass units) was calibrated for C₂F₄, C₂F₆, CF₃I, and C₂F₅I. For the first three gases it was nearly the same; for C₂F₅I it was about 20% higher. We assumed the response for the other products to be the same as for C₂F₅I. This certainly overestimates the yields of the heavier iodides. But because most of our products have low molecular weight, our quantitative results are hardly affected, with the exception of some distortion of the molecular weight distribution (Figure 6).

(5) Fuss, W. *Spectrochim. Acta* **1982**, *38A*, 829.

(6) Lewis, E. E.; Naylor, M. A. *J. Am. Chem. Soc.* **1947**, *69*, 1968.

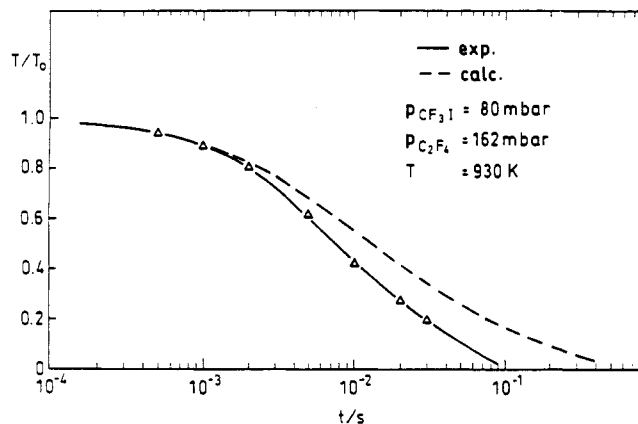


Figure 1. Time dependence of the temperature in cell A: (Δ) measured by the pressure probe; (---) calculated.

3. Calculation of Heat Conduction

Suppose a long cylindrical irradiated volume of radius r_b , which is much smaller than the cell radius, and with an initial temperature T_0 , which can be calculated from the absorbed energy. Its temperature evolution is approximately described for temperatures near T_0 by

$$\begin{aligned} T/T_0 &= (1 + 4\kappa t/r_b^2)^{-1} \exp(-r^2/(4\kappa t + r_b^2)) \\ &= (1 + 4\kappa t/r_b^2)^{-1} \quad \text{on the axis} \end{aligned} \quad (6)$$

κ is the temperature conductivity (heat diffusivity). It is related to the heat conductivity λ by

$$\kappa = \lambda/(c_p \rho) \quad (7)$$

where ρ is the density and c_p the specific heat of the gas. λ is nearly independent of ρ . The temperature dependence of κ is usually described by a power law with a small positive exponent i , which must be found from experiments:

$$\kappa/\kappa_{300\text{K}} = (T/300\text{K})^i \quad (8)$$

A temperature-independent κ has been assumed for derivation of (6). Therefore, (6) will be valid only for temperatures near T_0 . For the other calculations of heat conduction (see below), we took the temperature dependence of all quantities of (7) into account. κ is inversely proportional to pressure. The heat loss out of the volume V , containing the hot gas is (dot = time derivative)

$$\dot{Q} = \rho V c_p \dot{T} \quad (9)$$

For a given temperature c_p can be calculated from spectroscopic data. \dot{Q} is pressure independent and $\dot{T} \propto \rho^{-1}$. This follows already from the differential equation. So it is also true for more complicated heat conduction problems.

Most of our experiments have been done in a small cell, where neither the cylindrical wall nor the windows were far from the irradiated region. So the heat conduction equation had to be solved numerically. This was done by expanding the dependence on radius r and on the axial coordinate z into two series and writing the solution as a product of both:

$$(T - T_\infty)/(T_0 - T_\infty) = \sum_m A_m(r,t) \sum_n B_n(z,t) \quad (10)$$

The first factor is the usual solution for a long cylinder and the second one for a pair of infinitely large plates. For details of the method see refs 7–9 or for our case, ref 10.

The calculations were performed with various exponents in (8). The results were compared with the temperature evolution, derived from the measurements of pressure. An example is shown in Figure 1. The calculated curve in this figure corresponds to i

(7) Grigull, U.; Sandner, H. *Wärmeleitung*; Springer: Berlin, 1986.

(8) Eckert, E. R. G. *Einführung in den Wärme- und Stoffaustausch*; Springer: Berlin, 1966.

(9) Succi, James *Heat Transfer*; Simon & Schuster: New York, 1975.

(10) Gong, Mengxiang Doctoral thesis, University of Munich 1989; also available as Report MPQ 142, Max-Planck-Institut für Quantenoptik, Garching, 1989.

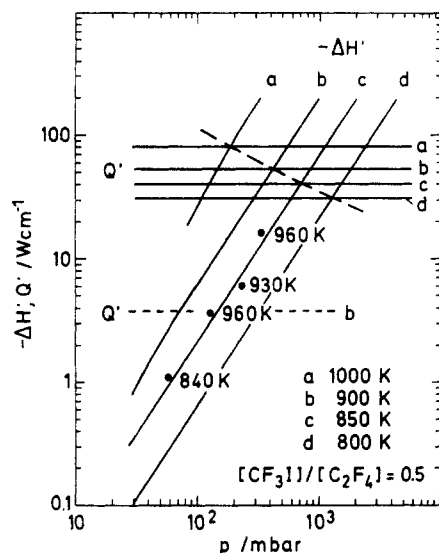
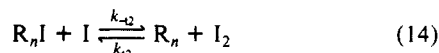
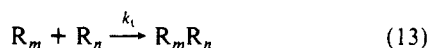
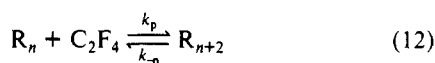


Figure 2. Heat loss \dot{Q} (solid lines, cell A; dots, cell C) and release of reaction enthalpy $-\Delta\bar{H}$ per unit length of the cell. \dot{Q} is based on calculations (numerical for cell A and according to eq 6 for cell C, beam radius $r_b = 8$ mm). The solid lines for $\Delta\bar{H}$ are calculated from eqs 25 and 22. The broken line indicates the expected ignition threshold. The experimental points are from measured conversions, divided by the time for cooling from the indicated initial temperatures to 800 K.

= 2. Exponents around 1 are common for light gases. An even better fit can be obtained if $\kappa_{300\text{K}}$ is also varied. We assumed, however, $\kappa_{300\text{K}} = 2.25 \times 10^{-2} \text{ cm}^2/\text{s}$ at 1 bar, which corresponds to a λ , intermediate between the values for CF_3I and some gases similar to C_2F_4 .¹¹ The cooling times, observed in the way of Figure 1, were proportional to pressure in the range investigated by the pressure probe (70–250 mbar).

4. Kinetics and Release of Heat of Reaction

For the total reaction velocity, important for the heat release, it is sufficient to consider one initiation reaction (thermal dissociation of CF_3I), one propagation reaction (molecule growth) and its reverse, one termination reaction, and the I_2 formation from I + an iodide. Denoting the radicals $\text{CF}_3(\text{CF}_2)_n$ by R_n , they are



The chain-transfer reaction



only determines the product distribution over n . The three-body recombination of I^{12} is too slow to compete with the high-temperature reaction (14). The rate constant for the termination reaction



is $\approx k_t$.¹³ Nevertheless it does not affect $[\text{R}]$, because reaction 14 efficiently reduces $[\text{I}]$. We found this by numerical integration

TABLE II: Conditions for Neglection of the Depolymerization^a

T/K	1200	1100	1000	900	800	700
$[\text{C}_2\text{F}_4]/\text{mbar} \geq$	6490	1360	210	21	1.2	3×10^{-2}

^aThe numbers result from the postulate $k_p[\text{C}_2\text{F}_4] \geq 10k_{-p}$. The concentration unit "mbar at room temperature" corresponds to 40 $\mu\text{mol/L}$.

of the rate equations, which included some n dependence of the rate constants and a series of additional reactions. But it can also be confirmed by assuming stationary concentrations for R_n , I , and I_2 and using the following rate constants (RT in kJ/mol):

$$k_i = 10^{13} \exp(-223/RT) \text{ s}^{-1} \quad (\text{ref } 14)$$

$$k_p = 10^8 \exp(-19.2/RT) \text{ L mol}^{-1} \text{ s}^{-1} \quad (\text{refs } 15, 16)$$

$$k_{-p} = 7.9 \times 10^{13} \exp(-191/RT) \text{ s}^{-1} \quad (\text{ref } 16)$$

$$k_t = 10^{10} \text{ L mol}^{-1} \text{ s}^{-1} \quad (\text{ref } 15)$$

$$k_{i_2} = 1.2 \times 10^9 \text{ L mol}^{-1} \text{ s}^{-1} \quad (\text{ref } 17)$$

$$k_{-i_2} = 4 \times 10^9 \exp(-67/RT) \text{ L mol}^{-1} \text{ s}^{-1} \quad (\text{ref } 17)$$

$$k_{tr} = k_{-tr} = 1.3 \times 10^8 \exp(-39/RT) \text{ L mol}^{-1} \text{ s}^{-1} \quad (\text{ref } 18)$$

The steady-state concentrations of R follow from

$$d[\text{R}]/dt = k_i[\text{CF}_3\text{I}] - 2k_{t1}[\text{R}]^2 = 0 \quad (17)$$

$$[\text{R}] = (k_i[\text{CF}_3\text{I}]/k_t)^{0.5} \quad (18)$$

Define

$$[\text{R}] = \sum_n [\text{R}_n] = \sum_n [\text{CF}_3(\text{CF}_2)_n] \quad (n \geq 0) \quad (19)$$

$$[\text{R}'] = \sum_n [\text{R}_n] = \sum_n [\text{CF}_3(\text{CF}_2)_n] \quad (n \geq 2) \quad (20)$$

Then the reaction rate

$$-d[\text{C}_2\text{F}_4]/dt = k_p[\text{R}][\text{C}_2\text{F}_4] - k_{-p}[\text{R}'] \quad (21)$$

$$\geq (k_p[\text{C}_2\text{F}_4] - k_{-p})[\text{R}] \quad (22)$$

Inserting the numbers, we get (concentrations in mol/L, time in s, RT in kJ/mol)

$$-d[\text{C}_2\text{F}_4]/dt \geq [\text{CF}_3\text{I}]^{0.5}([\text{C}_2\text{F}_4] \cdot 3 \times 10^9 \exp(-131/RT) - 2.5 \times 10^{15} \exp(-302/RT)) \quad (23)$$

$$-d[\text{C}_2\text{F}_4]/dt \approx [\text{CF}_3\text{I}]^{0.5}[\text{C}_2\text{F}_4] \cdot 3 \times 10^9 \exp(-131/RT) \quad (24)$$

In the latter form, the depolymerization was neglected. This is possible under the conditions listed in Table II. These conditions hold for most of our experiments.

If the initial temperature is deduced from the absorbed energy, we can calculate the reaction velocity and from this in turn the release rate of the reaction enthalpy by

$$\Delta H^* = \Delta H(-d[\text{C}_2\text{F}_4]/dt)V \quad (25)$$

V is the irradiated volume and $\Delta H = -159 \text{ kJ/mol}$.¹⁹ From (24) follows that, at a given total pressure p , $-d[\text{C}_2\text{F}_4]/dt$ and $-\Delta H^*$ should be maximum, if $[\text{CF}_3\text{I}]/[\text{C}_2\text{F}_4] = 0.5$. This ratio was used

(14) At most of our pressures we are still in the falloff region. For this reaction. Therefore, we took a value which is about 400 times smaller than the high-pressure limit given by: Saito, K.; Yoneda, Y.; Tahara, H.; Kidoguchi, S.; Murakami, I. *Bull. Chem. Soc. Jpn.* **1984**, *57*, 2661.

(15) Bamford, C. H.; Tipper, C. F. H. *Chemical Kinetics*; Elsevier: Amsterdam, 1976; Vol. 18.

(16) Rodgers, A. S. In *Fluorine containing free radicals, kinetics and dynamics of reactions*; Root, J. W., Ed.; ACS Symposium Series 66; American Chemical Society: Washington, DC, 1978; pp 296–313.

(17) Laurence, G. S. *Trans. Faraday Soc.* **1967**, *63*, 1155.

(18) This is the rate constant for $\text{CH}_3 + \text{CF}_3\text{I} \rightarrow \text{CH}_3\text{I} + \text{CF}_3$; Sidebottom, H.; Treacy, J. *Int. J. Chem. Kinet.* **1984**, *16*, 579.

(19) *JANAF Thermochemical Tables*, 2nd ed.; Stull, D. R., Prophet, H., Eds.; National Bureau of Standards: Washington, DC, 1971; NSRDS-NBS-37.

(11) Landolt-Börnstein. *Zahlenwerte und Funktionen—Eigenschaften der Materie in ihren Aggregatzuständen*; Band 2, Teil 5, Springer: Berlin, 1968.

(12) Kondrat'ev, V. N. *Chemical Kinetics of Gas Reactions*; Pergamon Press: Oxford, 1964.

(13) Skorobogatov, G. A.; Seleznev, V. G.; Slesar, O. N. *Dokl. Phys. Chem.* **1976**, *231*, 1292.

in most of our experiments. With this ratio fixed, at a given temperature $-d[\text{C}_2\text{F}_4]/dt$ (thus also $\Delta\dot{H}$) is proportional to $p^{3/2}$. Yields of products are equal to (reaction rate) \times (reaction time). The latter, equal to the cooling time, is $\propto p$. So the yields of the desired C₂F₄ addition products should grow as $p^{5/2}$. Absorption is $\propto p$, as long as it is low. Therefore, the quantum yields of the desired products should be $\propto p^{3/2}$ at low to intermediate pressures. The radicals combine at a rate $\propto [\text{R}]^2$. So the quantum yield of these products should be $\propto p^{3/2}$ at low to intermediate pressures. The yield ratio of the desired iodides over the radical dimers should therefore be $\propto p^{1/2}$. So the selectivity and the quantum yield both increase with pressure. This result is general, provided that propagation and termination reactions are respectively of first and second order in the radical concentrations, as in a very widespread type of chain reaction.

Some of these predictions have been verified by the experiments (section 6).

Figure 2 illustrates the predicted scaling of the enthalpy release $\Delta\dot{H}$ and the heat loss \dot{Q} with pressure and temperature. Above the broken line, $-\Delta\dot{H} > \dot{Q}$; i.e., ignition is expected. The $\Delta\dot{H}$ lines have been calculated by (25) and (23). To derive the experimental points of Figure 2, we divided the measured iodide yields by the measured times to cool from the indicated initial temperatures to 800 K (where the reaction practically stops) and multiplied this rough conversion rate by ΔH_V according to (25). Although this procedure can only be an order-of-magnitude check, the points deviate only by 50–100 K from the expected curve, and the pressure dependence agrees with prediction.

In larger cells, whose cold walls are far from the heated zone, the ignition threshold is expected at lower pressure. This is also indicated in Figure 2.

5. Kinetics at Low Pressure

At low pressure an initial concentration $[\text{CF}_3]_0$ is generated in a short time compared to the time of subsequent reactions. Then the time-dependent $[\text{CF}_3]$ follows from

$$-d[\text{CF}_3]/dt = k_p[\text{C}_2\text{F}_4][\text{CF}_3] + 2k_t[\text{CF}_3]^2 \quad (26)$$

From $\int_0^\infty [\text{CF}_3] dt$ one calculates the yields y_p of the C₂F₄ addition products. Using standard integral tables, one obtains

$$[\text{CF}_3] = [\text{CF}_3]_0 w [(1 + w) \exp(k_p[\text{C}_2\text{F}_4]t) - 1]^{-1} \quad (27)$$

$$y_p = k_p[\text{C}_2\text{F}_4] \int_0^\infty [\text{CF}_3] dt = [\text{CF}_3]_0 w \ln(1 + w^{-1}) \quad (28)$$

with

$$w = k_p[\text{C}_2\text{F}_4]/(2k_t[\text{CF}_3]_0)$$

For infrared multiphoton dissociation at low pressure (< 1 mbar) and high conversion ($> 10\%$), $w \ll 1$ is typical. In this case only a small fraction of CF_3 is converted to C_3F_7 . This radical is in part converted to $\text{C}_3\text{F}_7\text{I}$. The yield of this product iodide does not depend on w for $w \ll 1$, as shown in ref 10. The maximum yield of product iodides ($= [\text{CF}_3]_0$) is reached only for $w \gg 1$.

The yield of radical combination products follows from material balance

$$y_{\text{R2}} = 0.5([\text{CF}_3]_0 - y_p) = 0.5[\text{CF}_3]_0(1 - w \ln(1 + w^{-1})) \quad (29)$$

$$= 0.5[\text{CF}_3]_0 \quad \text{at } w \ll 1$$

$$= 0.5k_t[\text{CF}_3]_0^2/(k_p[\text{C}_2\text{F}_4]) \quad \text{at } w \gg 1$$

So at low $[\text{C}_2\text{F}_4]$ practically all $[\text{CF}_3]_0$ is consumed for dimerization. Only if $w \gg 1$, i.e., if

$$[\text{C}_2\text{F}_4]/[\text{CF}_3]_0 \gg k_p/2k_t = 2500 \quad \text{at room temperature} \quad (30)$$

a large part of $[\text{CF}_3]_0$ is converted to addition products.

6. Results and Discussion

Figure 3 shows the pressure dependence of quantum yield, of dissociation probability of CF_3I , and of product ratios, measured in various cells and at different energy densities. The quantum

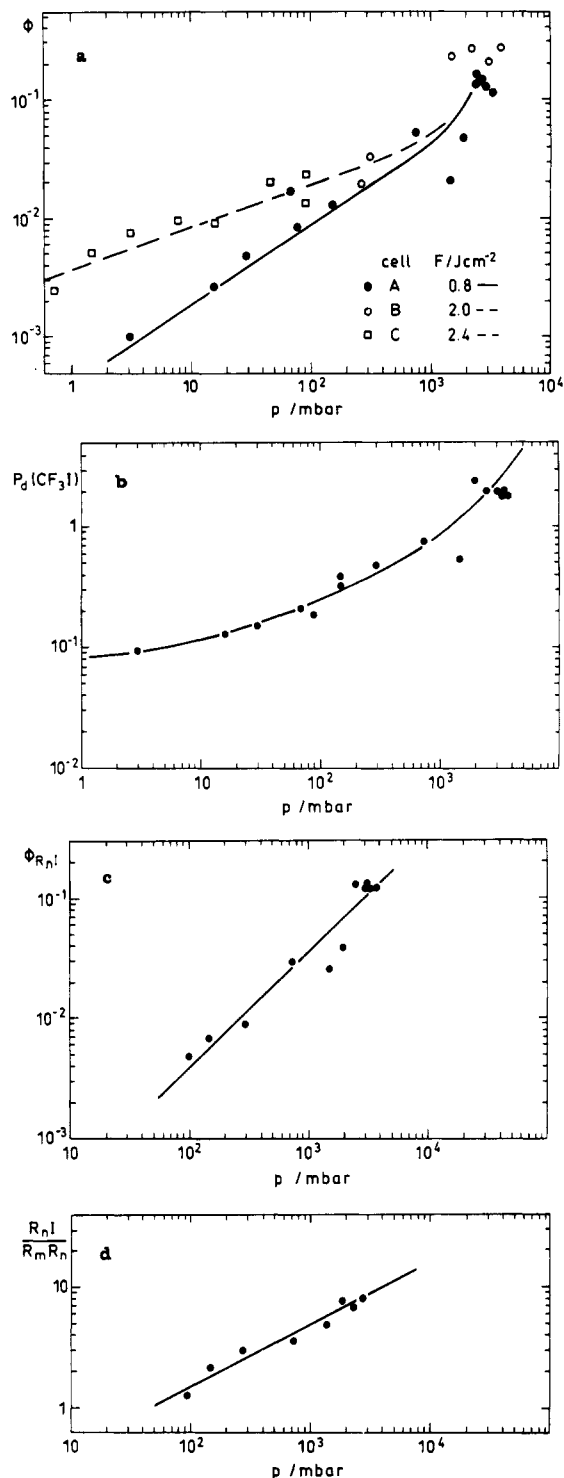


Figure 3. Quantum yields of converted CF_3I (a) and of iodide products (c), dissociation probability of CF_3I (b), and product ratio of iodide products to radical combination products (d). Abscissa is the total pressure p , $[\text{CF}_3\text{I}]/[\text{C}_2\text{F}_4] = 0.5$. Note that 25.0 mbar = 1 mmol/L at room temperature.

yield Φ of CF_3I conversion (Figure 3a) steadily grows with pressure. At 2–3 bar its increase seems to turn steeper. So probably in or near this pressure range is the ignition threshold. A clearer indication of ignition is the absolute Φ : In this pressure range, on the average only 3–5 photons have been spent to convert one CF_3I molecule. This is 4–6 times less than the dissociation energy. Another indication is the dissociation probability P_d which is > 1 at high pressures (Figure 3b). P_d is the ratio of molecules converted per pulse (in all the cell) over the molecules in the irradiated volume. For the latter we took the region until the e^{-1} penetration depth at high pressure, and the full cell length at low pressure.

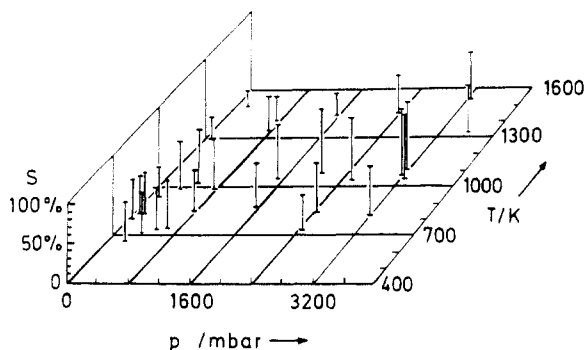


Figure 4. Selectivity S (yield of iodide products over converted CF_3I) versus total pressure p and temperature T . The figure should be considered as a three-dimensional perspective plot.

The penetration depth for our gas mixture is $l = 0.5p^{-1}$, l in cm, p in bar. So it is 1 or 10 cm (these are the lengths of the cells A and C, respectively) already at 500 and 50 mbar, respectively. For shorter and shorter penetration depths, the volume to surface ratio becomes more and more favorable for heat conduction and so unfavorable for ignition. This is certainly the reason why no clear threshold appears in Figure 3. This is also the case for the large diameter cell C, in which the heat loss is about 14 times slower than in cell A (see Figure 2), as long as its full length is illuminated. Because it is 10 times longer, the pressure threshold was again not reached.

For the large diameter cell, cooling by adiabatic expansion can also contribute. It occurs with the velocity of sound and, therefore, very rapidly. But after pressure equalization it stops. In cell C this corresponds to cooling from, e.g., 1000 to 890 K. So this effect can be easily compensated by using 11% more laser energy.

As mentioned in section 4, we expected $\Phi \propto p^{3/2}$ for the iodide products. The observed logarithmic slope is only about 1 at 0.8 J/cm² (Figure 3c) and even less at 2.4 J/cm² (not shown, but compare Figure 3a). Probably this is due to the assumption in section 4 of constant concentrations of CF_3I and C_2F_4 , whereas actually these gases were appreciably consumed (20–50% conversion) in the experiments (Figure 3c). But it is also possible that the consideration of temperature evolution was not detailed enough: If spatial propagation of the “flame” is taken into account, the result would probably be that it extinguishes even before it reaches the cold wall. In ratios of yields, the uncertainty about the reaction time (cooling time) and the effect of reagent consumption should disappear. Figure 3d shows that the ratio of desired to undesired product is $\propto p^{1/2}$, as predicted. So the kinetic analysis is basically correct.

Figure 4 shows the selectivity S (quantity of desired products over total conversion) as a function of pressure and initial temperature. S increases with pressure (at least for temperatures >1300 K), as mentioned in the Introduction and as predicted by the kinetic analysis. Common experience tells that the higher the temperature, the more side products should be expected. Figure 4 shows, however, that there is an initial rise of S until an optimum temperature and that this temperature increases with pressure. It turns out that this is just the (pressure dependent) temperature where depolymerization sets in according to eq 23. The radical combination products lose their importance at high pressure according to the dependence shown in Figure 3d (and predicted in section 4), and catastrophic decomposition (leading to CF_4 + carbon) sets in only at higher temperatures.

Figure 3d also demonstrates the poor selectivity S at low pressure. (The ordinate in this figure is $S - 1$.) Figures 3 and 4 apply to a fixed ratio of $[\text{C}_2\text{F}_4]/[\text{CF}_3\text{I}] = 2$. Increasing this ratio also improves S , because the addition of C_2F_4 to the CF_3 radical can then better compete with the radical dimerization. This is why Bagratashvili et al.³ used a large excess of C_2F_4 . Our data also show this possibility (Figure 5). However, this figure also shows that the quantum yields of the desired products do not increase in this way. This is similar to the case in which the radicals are generated in a time short compared to the time scale

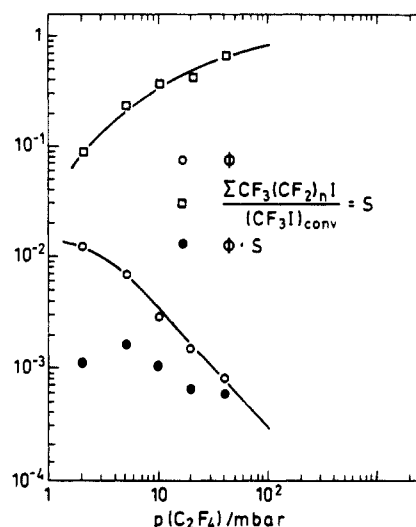


Figure 5. Quantum yield Φ of CF_3I conversion (open circles) and of iodide products (full circles) and selectivity S (open squares) versus C_2F_4 pressure. CF_3I pressure was 1 mbar.

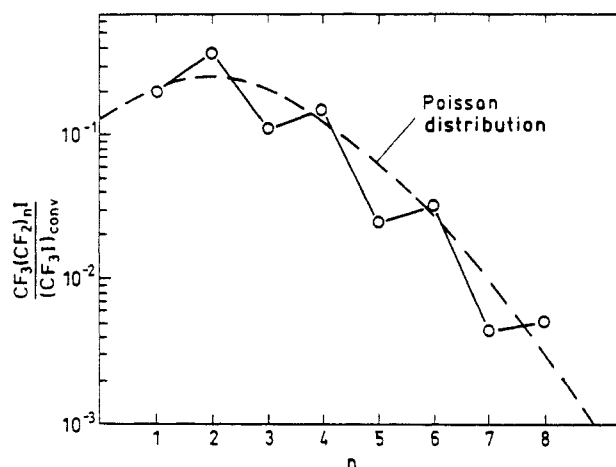
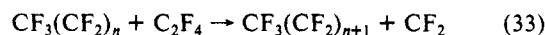
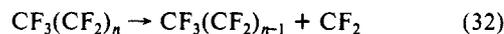
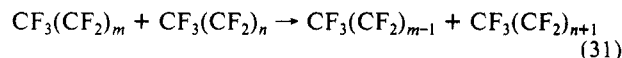


Figure 6. Distribution of product iodides $\text{CF}_3(\text{CF}_2)_n\text{I}$ over n . The pressures of CF_3I and C_2F_4 were 181 and 1410 mbar, respectively.

of the subsequent reactions (section 5). Kinetic analysis for this case predicted yields $\propto [\text{C}_2\text{F}_4]$. But the absorption increases in the same way in our case, because of collisional energy transfer to C_2F_4 during the laser pulse. We found that the ratio of products $\text{C}_2\text{F}_6/\text{C}_3\text{F}_7\text{I}$ agrees quantitatively with (27) and (29), if we use for k_p the temperature (850 K) calculated from laser absorption.

The dissociation probabilities at low pressures, found by us at the laser line 9P28 (0.08 at 0.8 J/cm² to 0.25 at 2.5 J/cm²), are consistent with previous data.²⁰

Figure 6 shows the degree of polymerization of the desired products. The products with odd n can obviously not be produced by the reaction scheme (11)–(15). A transfer of a CF_2 group takes place. Three reactions could bring it about:



The dissociation of C_2F_4 is too slow at our temperatures (see vol. 5 of ref 15). For radical concentrations that are typical for our conditions, it turns out that reaction 31 cannot be very important. Otherwise we should also observe more radical combination products. Reaction 32 is endothermic by about 330 kJ/mol. So

(20) Bagratashvili, V. N.; Dolzhikov, V. S.; Letokhov, V. S.; Ryabov, E. A. *Appl. Phys.* **1979**, *20*, 231. Bagratashvili, V. N.; Dolzhikov, V. S.; Letokhov, V. S.; Makarov, A. A.; Ryabov, E. A.; Tyakht, V. V. *Sov. Phys. JETP* **1979**, *50*, 1075.

it is probably also too slow. Reaction 33 is endothermic by only 59 kJ/mol. It is conceivable that the activation energy is not much higher. Therefore, we suggest it as a candidate to explain the exchange of CF_2 groups.

The CF_2 exchange is slow compared to the chain growth and chain transfer. Therefore, the n dependence of the yields are parallel for odd and even n . For the n dependence of the even n products, a Poisson distribution is expected, if each iodide product can enter again into the reaction sequence just like the starting iodide CF_3I .¹ Such a distribution is also indicated in the figure. But similar product distributions can also be expected, if $\log(\text{chain-transfer rate}/\text{chain-growth rate})$ decreases as $(n + 1)^{-2}$.¹ Such behavior is often observed and is interpreted as a consequence of electrostatic effects on the rate constants. Our data are not sufficient to distinguish the two mechanisms.

7. Conclusion

We obtained quantum yields Φ (produced $\text{CF}_3(\text{CF}_2)_n\text{I}$ molecules/absorbed photons) of up to 0.2 with selectivities S (produced iodide/converted CF_3I) up to 0.8. These results are much better than the previous ones ($\Phi \approx 10^{-3}$, $S = 0.1$), attained at low pressures. The success at high pressure is due to the fact that the radicals are consumed already while they are generated. So their concentration never grows large enough for dimerization. The high S is surprising in view of the high temperatures involved (more than 1000 K). S begins to drop again only at temperatures where a side reaction sets in. This is the reverse of the C_2F_4 addition, in our case. Therefore, the optimum temperature rises with pressure (Figure 4). That both S and Φ also rise with pressure is a consequence of the steady-state kinetics with propagation of first order and termination of second order (section 4). This is the most common type of chain reaction. If propagation and termination have the same kinetic order, S and Φ will not depend on pressure.

Although the application of kinetic principles allowed us to increase the quantum yield already by 2 orders of magnitude, an even higher Φ could be attained if the ignition condition $-\Delta\dot{H} \geq \dot{Q}$ were reached. The key problem consists in that the penetration depth became too small at the pressures of interest. The thin heated layer has a surface-to-volume ratio that favors heat conduction. In order to reach the ignition threshold, one should obviously use a wavelength that can penetrate 10 cm or more at superatmospheric pressures. This is possible in the 10- μm range, especially in the presence of a sensitizer (e.g., cyclo- C_4F_8 which is a common impurity in C_2F_4). However, this is more difficult than it seems. To heat more molecules requires more energy per cm^2 . Above about 5 J/cm^2 of a microsecond CO_2 laser pulse, windows begin to be damaged. A way out of this difficulty is to use pulses of about 1 ms length. The energy load (which is basically a thermal load) that a window can stand grows as the square root of the pulse length. Heat conduction (Figure 1) as well as convection takes place on a longer time scale. CO_2 laser pulses with 1 ms length are often applied in material processing.

On the other hand, it should be noted that it is hardly worthwhile to improve our quantum yields. At a cost of about 0.02 DM/mol of CO_2 laser photons (100- μs pulses),²¹ the laser's contribution to the product cost is only 0.10 DM/mol.

Acknowledgment. For the detailed kinetic calculation, we used a computer program of Dr. F. Rebrost, which he kindly made available to us. To Prof. Zhang Linyang we are indebted for many helpful and stimulating discussions and for his help in the initial experiments. For his helpful technical support we thank Mr. J. Hartmann.

Registry No. C_2F_4 , 116-14-3; CF_3I , 2314-97-8.

(21) Fuss, W.; Schmid, W. E. "Kohlenstoffisotopentrennung mit einem gutgeschalteten CO_2 -Laser"; Report MPQ 138, Max-Planck-Institut für Quantenoptik, Garching, 1988.

An Examination of Pathways for the Reaction of $\text{O}(^3\text{P})$ Atoms with $\text{FCO}(^2\text{A}')$ Radicals

J. S. Francisco* and A. Ostafin

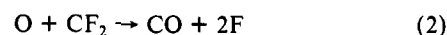
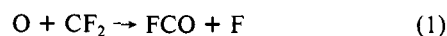
Department of Chemistry, Wayne State University, Detroit, Michigan 48202 (Received: November 6, 1989; In Final Form: March 1, 1990)

The reaction mechanism for the reaction of $\text{O}(^3\text{P})$ atoms with $\text{FCO}(^2\text{A}')$ radicals has been studied by means of ab initio quantum chemical techniques using polarized basis sets and including the effects of electron correlation and zero-point corrections. The mechanism involves the initial addition of $\text{O}(^3\text{P})$ to the $\text{FCO}(^2\text{A}')$ radical to form $\text{FC}(\text{O})\text{O}$ radicals, subsequently followed by fluorine elimination to form $\text{CO}_2(^1\Sigma_g^+)$. These results are consistent with experimental observations of Ryan and Plumb. The previously measured rate constant for the $\text{O}(^3\text{P}) + \text{FCO}(^2\text{A}')$ reaction is also suggested to be due solely to the following reaction which accounts for the loss of $\text{FCO}(^2\text{A}')$ radicals: $\text{O}(^3\text{P}) + \text{FCO}(^2\text{A}') \rightarrow [\text{FC}(\text{O})\text{O}]^{\ddagger} \rightarrow \text{F}(^2\text{P}) + \text{CO}_2(^1\Sigma_g^+)$.

Introduction

The increased use of fluorine-containing compounds in industrial processing has created the need for understanding the chemical processes taking place in these systems. One particular application has been their use in plasma etching of semiconductor devices. It has been observed that the addition of O_2 to CF_4 plasmas leads to enhanced rates of etching in single and polycrystalline silicon, and it has been concluded that this rate change is coupled with increases in excited fluorine atom concentrations,¹⁻³ which are considered to be the principal etchant species.

Detection of fluorine atoms, in the $\text{O}(^3\text{P}) + \text{CF}_3$ reaction as well as stable species such as CO , CO_2 , COF_2 , and SiF_4 has suggested the existence of a number of mechanisms for their formation in the plasma gas discharge. It has been proposed⁴ that the addition of O_2 results in the formation of fluorine, viz.



In the reaction between CF_2 and $\text{O}(^3\text{P})$ studied at 295 K in a gas flow reactor, the major by-product is found to be CO_2 , with some CO and COF_2 present in minor quantities. The possibility of CO_2 formation, viz.

(1) Flamm, D. L.; Donnelly, V. M. *Plasma Chem. Plasma Process* 1981, 1317.

(2) Jacob, A. U.S. Patent 3, 795, 597, 1974.

(3) Harshbarger, W. R.; Miller, T. A.; Norton, P.; Porter, R. H. *Appl. Spectrosc.* 1977, 31, 1977.

(4) Flamm, D. L.; Donnelly, V. M.; Ibbotson, D. E. *J. Vac. Sci. Technol.* 1983, B1, 23.